

A bypass wake induced laminar/turbulent transition

N.K. Kyriakides^a, E.G. Kastrinakis^a, S.G. Nychas^a, A. Goulas^b

^a *Department of Chemical Engineering, Aristotle University of Thessaloniki, 54006 Thessaloniki, Greece*

^b *Department of Mechanical Engineering, Aristotle University of Thessaloniki, 54006 Thessaloniki, Greece*

(Received 10 June 1998; revised and accepted 20 July 1999)

Abstract – The process of laminar to turbulent transition induced by a von Karman vortex street wake, was studied for the case of a flat plate boundary layer. The boundary layer developed under zero pressure gradient conditions. The vortex street was generated by a cylinder positioned in the free stream. An X-type hot-wire probe located in the boundary layer, measured the streamwise and normal to the wall velocity components. The measurements covered two areas; the region of transition onset and development and the region where the wake and the boundary layer merged producing a turbulent flow. The evolution of Reynolds stresses and rms-values of velocity fluctuations along the transition region are presented and discussed. From the profiles of the Reynolds stress and the mean velocity profile, a ‘negative’ energy production region along the transition region, was identified. A quadrant splitting analysis was applied to the instantaneous Reynolds stress signals. The contributions of the elementary coherent structures to the total Reynolds stress were evaluated, for several x -positions of the near wall region. Distinct regions in the streamwise and normal to the wall directions were identified during the transition. © 1999 Éditions scientifiques et médicales Elsevier SAS

laminar–turbulent transition / wake induced transition / turbulent production

1. Introduction

There are situations in aeronautics, process engineering and turbomachinery, where boundary layer transition originates from boundary layer interaction with transverse or longitudinal vortices (Squire [1]). The large scale motions of the wake exercise a considerable influence on the boundary layer and particularly on boundary layer transitions. An understanding of such transitional boundary layers can contribute to improvements in the design and operation of the corresponding equipment.

The natural transition process as it is described in Schlichting [2], is based on the formation, amplification and breakdown, due to instability of the Tollmien–Schlichting (T–S) waves. This process culminates with the formation and growth of turbulent spots, which finally coalesce into fully developed turbulent boundary layer flow. Morkovin [3] introduced the term ‘bypass transition’ to describe the transition process, which occurs in high disturbance flows, such as those present in turbomachinery. In the bypass transition process, the formation of turbulent spots may occur without the initial amplification of T–S waves observed in a natural transition. Kachanov [4] noted that the bypass transition is connected to direct non-linear laminar flow breakdown under the influence of external disturbances. This is observed when high enough levels of environmental perturbations (free-stream disturbances, surface roughness etc.) are present. Mayle [5], in his description of the various modes of transition, states that the effect of unsteadiness on transition, caused by the periodic passage of wake structures from upstream airfoils or obstructions (cylinders), is referred to as wake induced transition. According to Mayle, transition induced by wakes or shocks, compared to the above mentioned stages, appear to bypass the first stage of natural transition. The turbulent spots are formed and immediately coalesce, grow and propagate downstream.

Continued experimentation showed that the transition onset is strongly affected by the specific details of the free stream disturbance environment. This fact led to the introduction of the notion of receptivity by Morkovin [3]. Boundary layer receptivity was described as the response of the boundary layer to the influence of a strong disturbance of the environment, induced at the boundary layer. Much experimental work has been devoted to the study of the boundary layer receptivity (e.g., Schubauer and Skramstad [6]; Nishioka and Morkovin [7]; Goldstein and Hultgren [8]; Westin et al. [9,10]; Buter and Reed [11]). Westin et al. [9] studied experimentally the modification of the mean and fluctuating characteristics of a flat plate boundary layer subjected to nearly isotropic free stream turbulence. They arrived at certain conclusions concerning the parameters, which are relevant for the modeling of the transition process. Morkovin and Reshotko [12] proposed that there is no universality of the evolutionary path to the turbulent flow, because there is a large number of the disturbance environments and a variety of possible behaviours.

Squire [1] in a review of boundary layer/wake interaction, has indicated that the upstream wake increases the overall turbulence level in the flow and thus brings the transition process forward. As the wake moves closer to the surface, on which the boundary layer develops, the interaction begins earlier. On a more fundamental basis, Savill and Zhou [13] made an extensive study at low Reynolds numbers of various types of simple interactions, using flow visualization. These studies included interactions with a variety of wakes. Wakes formed behind a circular cylinder were examined, in order to obtain an essentially two-dimensional vortex street, with most of the turbulent energy contained in the highly coherent vortices. They studied what they called “slow” or “weak” interactions, in which the wake was initially sufficiently far from the boundary layer and was effectively fully developed, before it started to merge with the boundary layer. In contrast to this type of transition, “fast” or “strong” interactions, as they called them, were also studied. In this type of interaction, the initial vortex street is still present, when the two shear layers merge together. Savill and Zhou concluded that, the main parameter governing the growth of the interaction is the level of turbulence in the interaction region. Voke and Yang [14] performed a large eddy simulation of bypass transition on a flat-plate boundary layer; the free-stream turbulence level was considered 6%. Their simulation was in agreement with experimental data. They were able to predict the position and length of transition as well as aspects of the mechanism of the process.

Kyriakides et al. [15] studied experimentally the process of laminar to turbulent (L/T) boundary layer transition, induced by a von Karman vortex street wake. The boundary layer was developed on a sharp leading edge flat plate and the wake by a circular cylinder. Hot-wire measurements over a range of Strouhal frequencies and free stream velocities were carried out in order to identify the transition onset. From the analysis of the experimental data, the two different kinds of transition, mentioned above as “strong” wake and “weak” wake induced transition (Savill and Zhou [13]), were identified. A correlation for the prediction of the onset of the transition was proposed. The end of the strong wake induced transition was defined at the streamwise position, where the developing wake of the cylinder meets the wall. Furthermore Kyriakides et al. [16] investigated this strong wake-induced L/T-transition on a flat plate from the point of view of coherent structures. An X-type hot wire probe measured the streamwise and normal to the wall velocity components, while a gradient hot-wire probe, located in the cylinder’s wake and at the same streamwise position as the X-type hot wire probe, detected the passage of the von Karman vortices. From the simultaneously acquired velocity and gradient signals, the cross correlation functions, combined with a quadrant splitting analysis, were computed. Furthermore an ensemble average technique was applied to the signals. The analysis of the signals revealed, that during the transition a secondary vortical structure occurs near the wall.

The present work is a continuation of the work of Kyriakides et al. [15,16]. The hot-wire anemometry measurements allowed the evaluation of the contributions of the elementary coherent structures (ejections, sweeps, interactions wallward and interactions outward) to the total Reynolds stress. A negative energy production region along the boundary layer transition region was identified. The development of this negative

energy production region close to the wall, was studied using the Reynolds stress distributions and the corresponding contributions to the Reynolds stress of the elementary coherent structures.

2. Experimental facility

The experiments were conducted in a low speed boundary layer wind tunnel at a free stream velocity of $U_0 = 5$ m/s. A general view of the experimental arrangement is given in *figure 1*. The free stream turbulence intensity, Tu , in the wind tunnel was about 0.4% ($Tu = (\overline{u^2})^{1/2}/U_0 = 0.004$). From the velocity measurements, a friction velocity, u_τ , was obtained in the following way. By trial and error and by applying the logarithmic velocity distribution for fully developed turbulent flow, a friction velocity of the order of 25 cm/s was determined; this value corresponds to the friction velocity just after transition has been completed. This is an indicative value and it is used solely for the presentation of the transitional data in a non-dimensional form. The working section of the wind tunnel had a cross section of 0.6×0.6 m² and a length of 2 m. The transition process was studied on a 1.24 m long aluminum flat plate of 10 mm thickness with a sharp leading edge (radius 0.5 mm). The plate was positioned at an incidence angle of -0.5° in order to avoid leading edge separation; it spanned the whole test section width of 0.6 m and it was positioned at 30 cm above the bottom of the test section. The plate was mounted on an independent supporting system, which was installed outside the tunnel; the system was provided with vibration insulating elements. In this manner, vibrations of the wind tunnel walls were not transmitted to the plate as it was nowhere in contact with the tunnel itself.

A cylinder with a diameter of $d = 10$ mm positioned upstream and parallel to the leading edge of the plate, was used to generate a two-dimensional wake, which interacted with the flow above the flat plate and the developing boundary layer. The cylinder was placed at the position $x_c = -10$ mm and $y_c = 25$ mm from the leading edge of the flat plate. Special precautions, as proposed by Van Atta and Gharib [17], were taken in order to avoid cylinder vibrations. According to Van Atta and Gharib, a vibrating cylinder develops a vortex street with unpredictable differences in the Strouhal frequency and a wake which is unsteady. In the present experiments, the formation of a steady state wake was necessary. This was assured by examining the velocity energy spectra, which had a single peak at the Strouhal frequency corresponding to the free stream velocity, where the measurements were carried out.

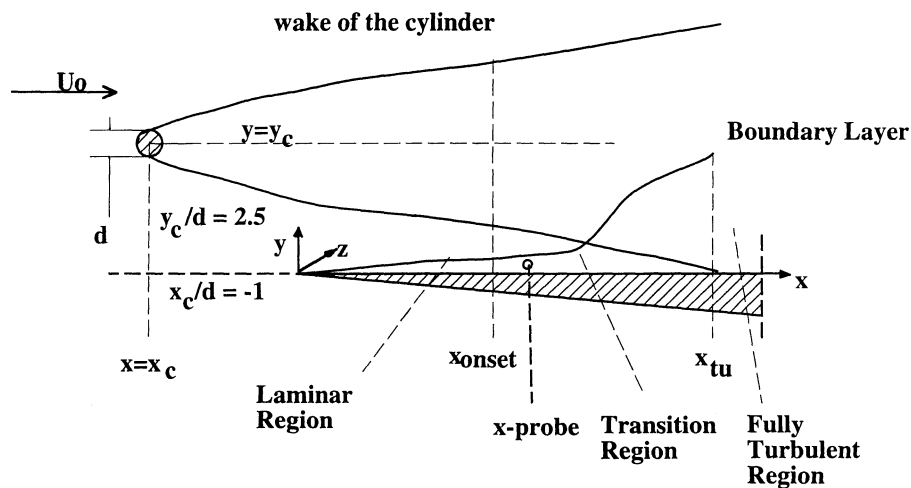


Figure 1. A general view of the experiment.

An X-type hot-wire probe (Dantec 55P53) was used for the simultaneous measurement of the streamwise velocity component, U , and velocity component normal to the wall, V , at various (x, y) positions in the boundary layer. All hot-wire measurements were conducted along the symmetry plane of the flat plate at various y -positions. Two manually controlled traversing mechanisms, with a total displacement of 20 cm in the streamwise direction and 20 cm in the normal direction and with an accuracy of 0.01 mm, were used for the x - and y -traversing of the hot wire probe. A supplementary traversing mechanism with an accuracy of 0.5 mm was used only for the longer x -displacements of the whole system. The calibration of the X-type hot-wire probe was carried out in the test section of the wind tunnel; during the calibration the cylinder was removed. The instantaneous signals from the probe were acquired simultaneously, for the various x -positions along the plate. Two constant temperature anemometers (Dantec 55M01) were used. The hot wire signals passed through a DC-offset controller, a gain amplifier and a low-pass filter, before being digitized by a 16-bit resolution A/D-converter. The duration of the data acquisition at each position was 12.5 s and the corresponding sampling frequency was 4 kHz. This duration was proved to be adequate for the proper statistical analysis of the signals. The probe position closest to the wall was specified by positioning underneath the probe tip a standard microscope glass plate of 0.2 mm thickness. All other distances from the wall were referenced with respect to that position. Therefore the accuracy of the absolute y -position was of the order of 0.1 mm. Alternatively the relative y -positions were accurate to within ± 0.01 mm (accuracy of the traversing mechanism).

Errors in the measurements due to the calibration procedure were taken into account. Drifting of the X-type hot-wire probe due to temperature variation or other factors was monitored by calibrating before and after a specific measurement. In this manner this error was kept to levels of about 1% for each velocity component. Another source of error examined was the one due to heat losses because of the proximity of hot-wire sensors to the wall of the aluminum plate. This kind of error has been examined, among others, by Wills [18] and Oka and Kostic [19]. For the closest distance of 0.7 mm measured here, the estimated error was negligible. Measurements with all standard X-type hot-wire probes are influenced by the velocity gradients and the error introduced are larger close to solid walls. For the present measurements error estimates for the closest to the wall distance of 0.7 mm have been carried out based on the influence of the $\partial U / \partial y$ -gradient and the analysis presented in Eckelmann et al. [20], Vukoslavcevic and Wallace [21] and Kastrinakis and Eckelmann [22]. Concerning the instantaneous streamwise velocity component, the maximum relative error based on the mean streamwise velocity, \bar{U} , was estimated to be up to 10%. Regarding now the local mean \bar{U} , this was independently measured with a single boundary layer probe (Dantec 55P15) and for the closest to the wall distance; these measurements differed from the corresponding X-probe data to around 1%. Concerning the instantaneous normal to the wall velocity component, v , the corresponding error based on the maximum instantaneous v was estimated to be up to 30%. This error, however, decreases rapidly with increasing wall distance, as shown in the above cited references.

3. Results and discussion

From the measured signals of the streamwise and normal to the wall velocity components, $U(t)$ and $V(t)$, respectively, at various (x, y) -positions, the corresponding mean velocities, \bar{U} and \bar{V} , were computed. Furthermore, from the fluctuating velocity signals $u(t)$ and $v(t)$, their rms-values, the instantaneous signals of the transfer terms $uv(t)$, $v^3(t)$ and $u^2v(t)$ and their mean values, were evaluated.

3.1. Characteristics of the undisturbed boundary layer and cylinder wake

Before starting the measurements on the process of the wake induced L/T-transition, the boundary layer characteristics without the presence of the cylinder and the cylinder wake characteristics as well, were separately studied at the free stream velocity of 5 m/s. In the case of the undisturbed boundary layer, detailed investigations showed, that it remained laminar, at least up to a streamwise distance of 1000 mm from the leading edge of the plate. The measured boundary layer velocity profiles are in agreement with the Blasius laminar velocity profile (Kyriakides et al. [15]). The maximum turbulence intensity levels within the boundary layer for all x -positions between $x = 0$ and $x = 1000$ mm, varied from 1 to 5% based on the local velocity. The shape factor $H = \delta_1/\delta_2$ (δ_1 is the displacement thickness and δ_2 the momentum thickness of the boundary layer) was always equal to 2.6, indicating that the boundary layer was still laminar. The present results are in agreement with the results of Schubauer and Skramstad [6] and Hall and Hislop [23]; they found that the critical Reynolds number for the natural transition onset was about $1.34 \cdot 10^6$.

The vortex street was generated using a cylinder of diameter $d = 10$ mm. The cylinder Reynolds number $Re = U_0 d / \nu$ was 3500; this implies that the cylinder wake was turbulent. Measurements were first carried out in the undisturbed wake of the cylinder. Within the cylinder wake and for several x/d and y/d positions, two velocity components U and V were measured using an X-type hot-wire probe. The measured mean velocity profiles, were in agreement with the velocity profiles of a two-dimensional wake behind a cylinder, as given by Schlichting [2]. Selected wake characteristics are presented in *table I*, together with the corresponding quantities in the presence of the flat plate for comparison. The data of this table show that the interaction of the cylinder wake with the boundary layer has decreased the $v_{\text{rms}} = (\overline{v^2})^{1/2}$ and increased the $u_{\text{rms}} = (\overline{u^2})^{1/2}$. A drastic increase of the values of the Reynolds stress is also observed due to the wake/boundary layer interaction. The characteristic shedding frequency of the wake could be clearly detected up to a distance of $x/d = 80$ –100 downstream of the wake origin, which is in agreement with the results of Cimbalá et al. [24];

Table I. Selected cylinder wake characteristics with and without the presence of the flat plate at various streamwise positions.

$d = 10$ mm		Without plate			With plate		
x/d	y/d	u_{rms}/U_0	v_{rms}/U_0	$100\overline{uv}/U_0^2$	u_{rms}/U_0	v_{rms}/U_0	$100\overline{uv}/U_0^2$
3	1.3	0.131	0.134	0.293	0.136	0.124	0.769
3	0.9	0.064	0.068	0.022	0.061	0.053	0.108
3	0.3	0.025	0.026	0.003	0.032	0.014	0.023
6	1.3	0.133	0.165	0.423	0.134	0.147	0.776
6	0.9	0.093	0.112	0.237	0.093	0.098	0.418
6	0.3	0.037	0.042	0.018	0.053	0.028	0.064
15	1.3	0.112	0.131	0.178	0.099	0.105	0.387
15	0.9	0.089	0.105	0.138	0.084	0.080	0.263
15	0.3	0.061	0.078	0.087	0.084	0.050	0.009
20	0.9	0.085	0.094	0.119	0.078	0.069	0.101
20	0.3	0.062	0.071	0.084	0.086	0.050	0.078
100	1.3	0.036	0.031	0.032	–	–	–
100	0.3	0.035	0.029	0.039	–	–	–
100	–1.5	0.025	0.021	0.021	–	–	–

further downstream the wake decayed. The autocorrelation functions of the U velocity signal were sinusoidal for distances shorter than $x/d = 30$. The Strouhal frequency, f_{st} , was equal to 95 Hz and the corresponding Strouhal number, St , was equal to 0.19.

3.2. The negative energy production region and turbulent kinetic energy transfer terms

In the present measurements the transition onset was observed at $x = 33$ mm from the sharp leading edge of the flat plate. The onset of the transition process was identified from the detailed observation of the U -velocity signal near the wall (at $y = 0.7$ mm). The velocity signals at various streamwise locations can be directly used to observe the changes of the flow near the wall, due to the laminar/turbulent transition. Before transition the velocity signal was sinusoidal with the Strouhal frequency of the cylinder. The amplitude of the sinusoidal velocity signal was amplified with the streamwise distance. At a certain streamwise distance the sinusoidal character of the streamwise velocity changes and additional non-periodic velocity fluctuations appear in the signal. This point is considered to be the onset of the L/T-transition. Further downstream the velocity fluctuations were amplified and the flow became turbulent. The power spectral density distributions close to the wall and for various x -positions showing the variation of the Strouhal frequency in the transitional boundary layer, were evaluated. The power level of the Strouhal frequency, beyond the position where the wake boundary came in contact with the laminar boundary layer, decreases drastically. This information concerning the power spectra can be found in Kyriakides et al. [15]. The end of transition is considered to be at the position downstream at which the turbulence intensity reaches a nearly constant level (Pfeil et al. [25]). For this work, as it is shown in *figure 2*, the product of the rms-values of u and v velocity fluctuations, $u_{rms} v_{rms}$, in the wall region increased constantly with streamwise distance and leveled off to the value of $(u_{rms} v_{rms} / U_0^2) \times 100 \approx 0.55$ at a streamwise distance corresponding to a Reynolds number $Re_x \approx 50000$. The data in *figure 2* show that at the distance where Re_x is about 67000 the transition process seems to have been completed. In addition, the intermittency factor was determined from the streamwise velocity component at $y = 0.7$ mm along the plate (Kyriakides et al. [16]). The data show that the intermittency factor reached the value one (1.0) for $x \geq 190$ mm. The type of transition is a strong wake induced transition, as was reported by Kyriakides et al. [15]. In that study it was established that the onset of the strong von Karman wake induced transition was a function of the free stream velocity, the position of the cylinder with respect to the plate, the cylinder diameter, the drag coefficient and the minimum velocity in the developing wake at the streamwise position of the onset of the boundary layer transition.

Figures 3 and 4 show the evolution of the profiles of the rms-values of u and v velocity fluctuations at several streamwise positions along the transition. Concerning the u_{rms} -profiles closer to the wall, they appear to be self-similar; the self-similarity of the profiles away from the wall ($y^+ > 200$) are attributed to the influence of the cylinder wake. The profiles indicate that a maximum occurs near the wall. The exact values and positions of these maxima cannot be established from our measurements. Furthermore, these profiles exhibit minima and the values of these minima vary linearly with the distance from the wall and up to a Re_x of about 35000. These minima occur at y^+ -distances from 15 to about 45 wall units. The minima of u_{rms}/U_0 , vary also linearly with streamwise distances up to Re_x of approximately 35000. In Kyriakides et al. [16] it was concluded that during the strong wake induced transition, a secondary structure is formed near the wall, simultaneously with the passage of the wake vortex with negative vorticity. This secondary vortical structure possesses positive transverse vorticity, it starts forming at the transition onset, it grows initially in scale and at a streamwise location corresponding to a Re_x of about 38500 ($x = 110$ mm) is lifted up. The scale of the secondary structure increases almost linearly with Re_x from about 15 wall units at $Re_x = 17500$ to about 45 wall units at $Re_x = 38500$. This scale suggests that there is a close association between the minima of u_{rms}/U_0 in *figure 3* and the passage of the secondary vortical structure. The maxima of u_{rms} -profiles observed in the

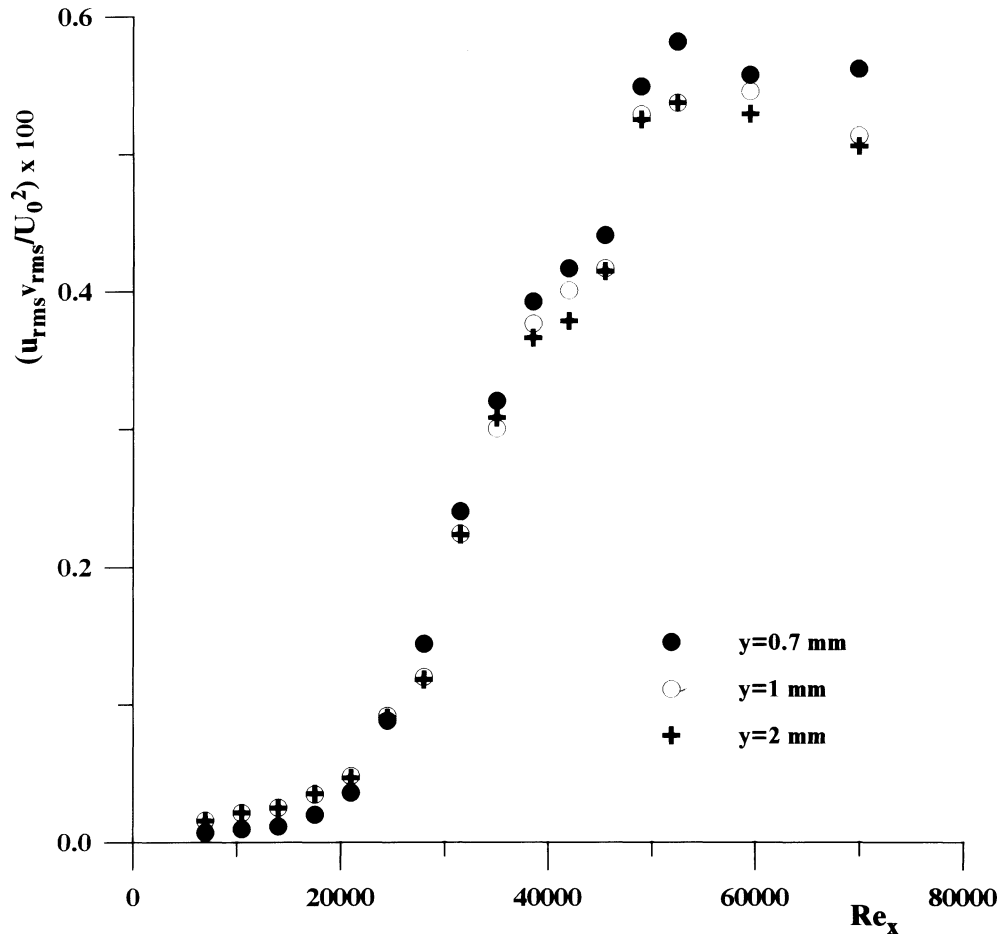


Figure 2. The product $u_{rms} v_{rms}$ along the transition region for three distances close to the wall.

outer region are also the result of the influence of the cylinder wake. Concerning now the profiles of the v_{rms} in figure 4, they appear also to be self-similar; they show an inflection point at around $y^+ = 25$. The rapid increase of the v_{rms} -values from the wall to the outer region is also attributed to the influence of the wake. In addition, table I shows that normal to the wall v_{rms} -fluctuations of the free stream are damped due to the presence of the wall. This is in agreement with the work of Voke and Yang [14].

Westin et al. [9] investigated the structure and receptivity in a boundary layer to a free stream of fairly isotropic turbulence with a turbulence level, v_{rms}/U_0 , varying from 1.35 to 1.5%. They reported measurements of u_{rms} -profiles at various downstream positions along the transition region; these profiles show a near self-similar behaviour. A comparison of the present work with the work of Westin et al. is in order. They observed that nearly isotropic free stream turbulence leads to perturbations in the boundary layer, which are dominated by large scale longitudinal structures growing downstream in scale. In their work, the u_{rms} -profiles are self-similar in shape and grow linearly downstream in amplitude. The apparent similarity between those findings and the ones of the present work should be viewed with caution because of the following differences between the two studies. The free stream turbulence in the present work is a highly structured wake, a von Karman vortex street, in contrast to the isotropic free stream of Westin et al. The characteristic wall structure in the present work,

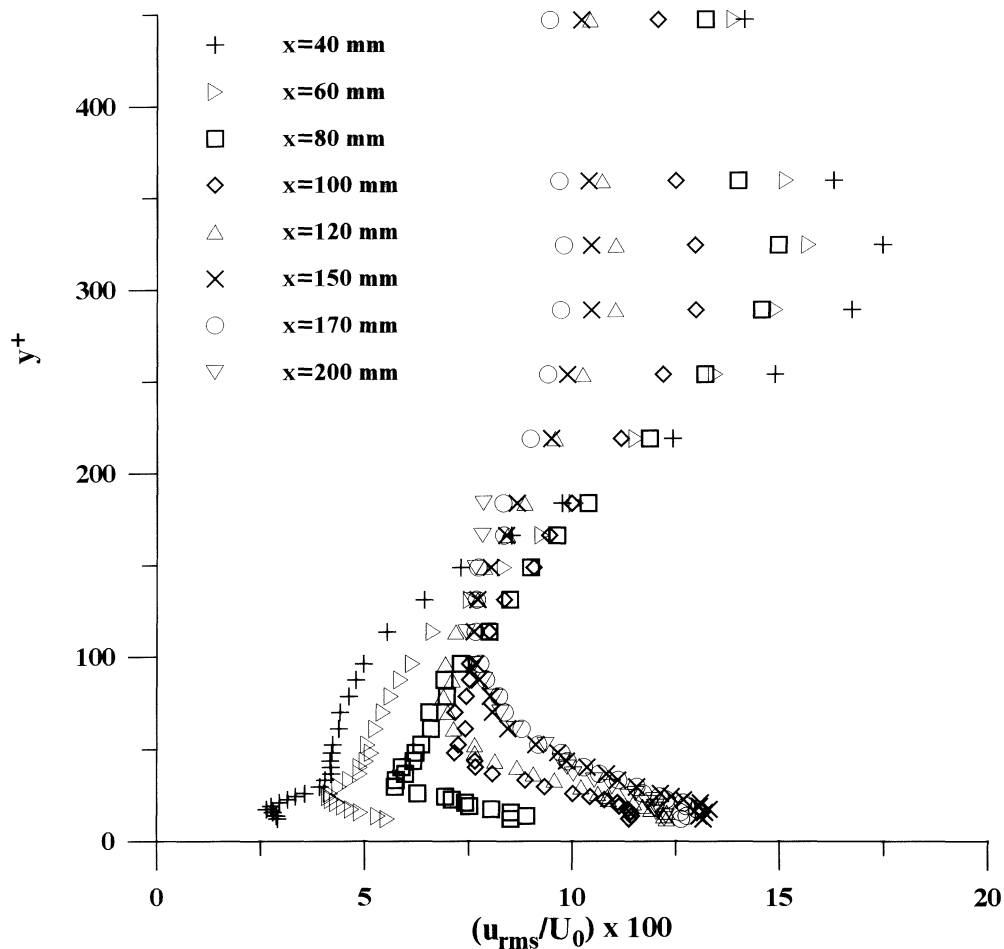


Figure 3. Profiles of the u_{rms} along the transition region.

which appears as the result of the receptivity of the boundary layer, is a transverse vortical structure in contrast to the longitudinal large scale structures referred in Westin et al. [9].

Concerning a comparison of the present study with the numerical study of bypass transition of Voke and Yang [14] the following points are mentioned. There is a qualitative agreement concerning the self similar behaviour of the u_{rms} -profiles close to the wall, regarding the maxima around y^+ of 20. Going further away from the wall, the behaviour of the u_{rms} is different and definitely influenced by the cylinder wake, as can be seen in figure 3, where between $y^+ \approx 200$ and 400 the self-similarity of the cylinder wake is clearly observed. Regarding now the v_{rms} in figure 4, there is a qualitative agreement between the two studies, again for the region close to the wall and also concerning the appearance of an inflectional profile. The influence of the cylinder wake is also clearly evident for the v_{rms} away from the wall. Regarding the question of receptivity of the laminar boundary layer, the present data also show the important role of the normal to the wall velocity fluctuations. Specifically the decrease of the v_{rms} and the increase of the u_{rms} as a result of the presence of the wall has already been mentioned (table I).

An overall picture of the boundary layer/cylinder wake interaction could be obtained by studying the \overline{uv} -profiles. Figure 5 shows mean velocity profiles and \overline{uv} -profiles for several streamwise positions normalized

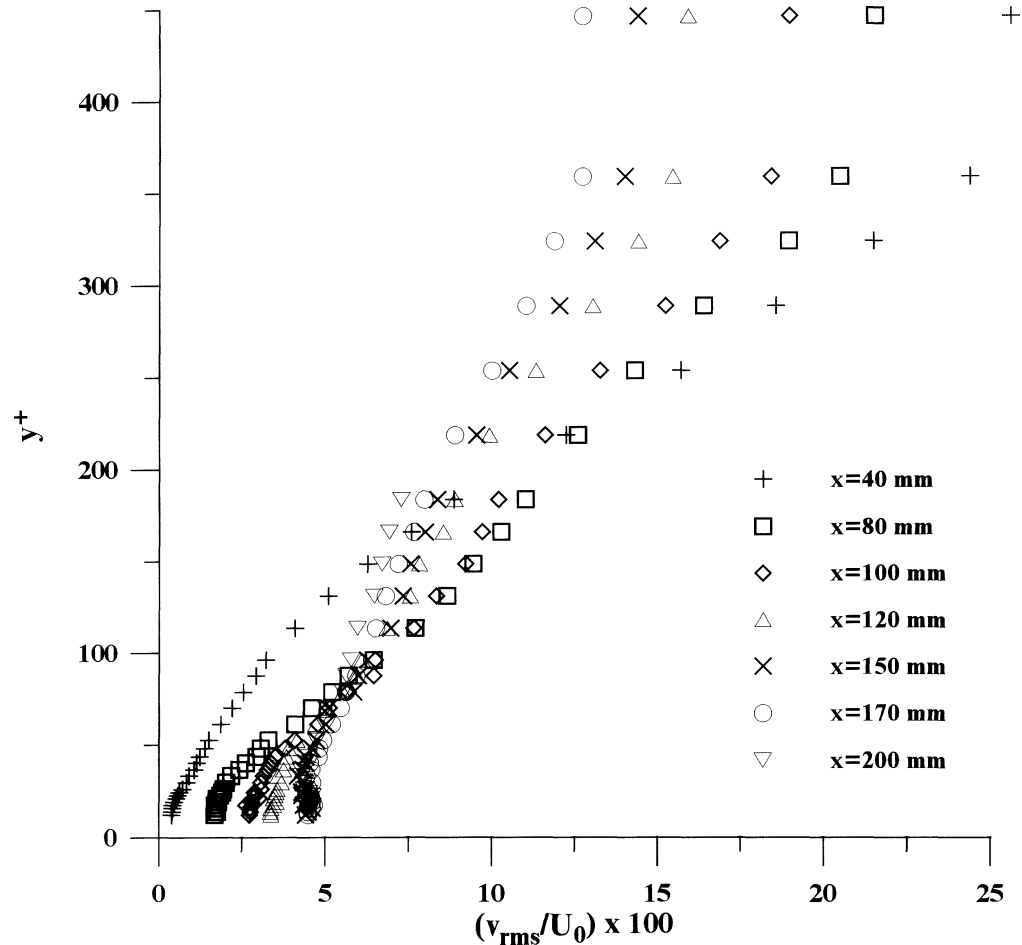


Figure 4. Profiles of the v_{rms} along the transition region.

with the free stream velocity, U_0 , and the squared free stream velocity, U_0^2 , respectively; pretransitional mean velocity profiles were presented in Kyriakides et al. [15] and they will not be repeated here. The x - and y -positions were made dimensionless by using the friction velocity, u_τ and the kinematic viscosity of the air, ν , according to the relations $x^+ = xu_\tau/\nu$, $y^+ = yu_\tau/\nu$. A local maximum of positive values of \overline{uv}/U_0^2 appears along the transition region, away from the wall at distances greater than about $y^+ = 400$ (not shown in figure 5); these maxima are attributed to the effect of the wake behind the cylinder. As can be seen in figure 5, along the transition region, there is a local minimum in the \overline{uv}/U_0^2 -distribution near the wall, the y^+ -position of which increases with streamwise distance. The value of this minimum is around zero up to a distance of $x = 100$ mm and becomes negative for greater x -positions along the transition region. The y^+ -extend of these negative \overline{uv}/U_0^2 -regions increases with streamwise distance. Regarding the Reynolds stress, the present data are compared with computations and data in Voke and Yang [14]. For their Reynolds number of $Re_x = 62900$, the minimum shown in their computation is $\overline{uv}/U_0^2 = -0.0012$; in the present case for $Re_x = 59500$ the minimum value of \overline{uv}/U_0^2 is about -0.0013 . There is an agreement for that particular case. It must be kept in mind, however, that the comparison regarding the \overline{uv} cannot be extended to the other cases, because the nature of their free stream (turbulence behind grids) is different from the present case, which is a turbulent wake (a highly structured flow) interacting with a boundary layer.

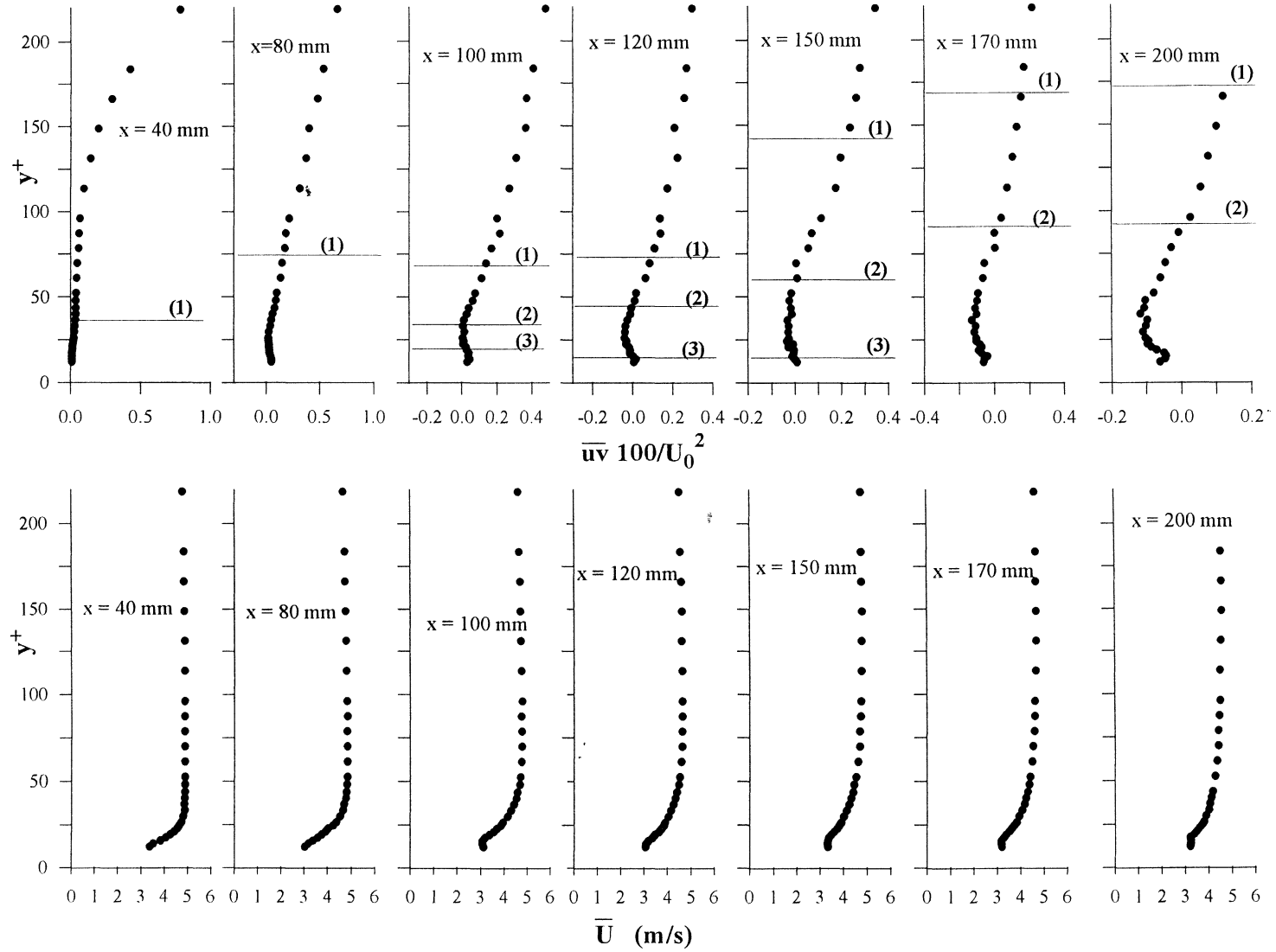


Figure 5. \overline{uv}/U_0^2 -distributions and mean velocity profiles for several streamwise locations.

In the y^+ -region of negative Reynolds stress, the gradient $d\bar{U}/dy$ was always positive, as can be deduced from the measured time averaged streamwise velocity profiles, shown in *figure 5*. Since the turbulent energy production is given by the term $-\overline{uv}d\bar{U}/dy$, it is positive in this region and consequently turbulent energy is produced. The y^+ -distance at which the local minimum of \overline{uv}/U_0^2 appeared, increases with the streamwise distance x^+ . For the \overline{uv}/U_0^2 profile at $x = 200$ mm, where the boundary layer was turbulent, the local minimum was observed at $y^+ = 37$. The solid line (1) in *figure 5* indicates the y -distance, where the gradient $d\bar{U}/dy$ becomes equal to zero. Furthermore, in all distributions of \overline{uv}/U_0^2 the solid lines (2) and (3) indicate the y -distances, where the Reynolds stress becomes equal to zero. The region between the solid lines (2) and (3), for every streamwise distance, is the production region of the wall. For the streamwise positions between $x = 33$ and 90 mm, the y^+ -region between the solid line (1) and the wall, which is characterized by $\overline{uv} > 0$ and $d\bar{U}/dy > 0$, is the “negative energy production region” or “the region of energy reversal”. For streamwise distances longer than $x = 100$ mm, the negative energy production region is located between the solid lines (1) and (2), which means that for $x > 100$ mm ($x^+ = 1750$) the negative energy production region is lifted away from the wall with increasing streamwise distance. The maximum width of the negative energy production region of about $y^+ = 80$ was observed at the location $x = 200$ mm ($x^+ = 3500$), where the flow becomes turbulent. It should be noted that according to the turbulent energy cascade process, turbulent kinetic energy is transferred from the mean flow to the velocity fluctuations. In the case of the negative energy production region the above consideration is not valid any more. Now, turbulent kinetic energy should be transferred from the fluctuations to the mean flow, reversing the cascade process, which in this case would mean transfer of energy from the small to the large scales.

As an example, in *figure 6* are presented the distributions of \overline{uv} , $\overline{v^3}$ and $\overline{u^2v}$ in the y -direction, normalized with the local rms-values of u and v , for the streamwise distance $x = 120$ mm. The regions which were defined by the lines (1), (2) and (3) in *figure 5*, coincide with the corresponding ones in the distributions of $\overline{v^3}$ and $\overline{u^2v}$.

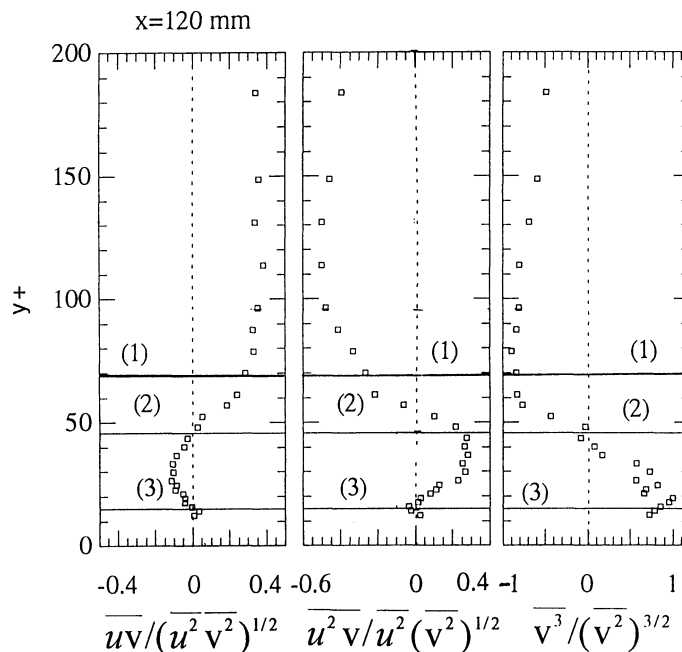


Figure 6. Normalized Reynolds stress and normalized turbulent kinetic energy transfer terms $\overline{u^2v}$ and $\overline{v^3}$ as a function of y^+ , at the streamwise position $x = 120$ mm.

in figure 6. The terms $\overline{v^3}$ and $\overline{u^2v}$, which present turbulent kinetic transfer in the y -direction, obtained negative values in the negative energy production region (between lines 1 and 2) and positive values in the production region. In this way, the change in the sign of $\overline{v^3}$ and $\overline{u^2v}$ with the y distance, could be considered as an indication of the turbulent kinetic energy transfer in the y -direction towards the wall. These findings are in qualitative agreement with the results from the Large Eddy Simulation of Voke and Yang [14] concerning the important role of wall normal free stream velocity fluctuations. Their computations show that external normal to the wall motions are converted into boundary layer streamwise motions. From this point of view the importance of the normal velocity component is manifested in our data by the high contribution of this component concerning the transfer of turbulent kinetic energy towards the wall. On the other hand concerning the production of turbulent kinetic energy, our data indicate a role of the normal fluctuations as negative contributors to this production (wallward interactions, see Section 3.3).

Bario et al. [26] and Squire [1], studied flat plate boundary layer/wake interactions and the development of the negative energy production regions, close to the wall of the plate. They suggested that, in all cases of this interaction, turbulent kinetic energy was transferred from the negative energy production region to the production region. Bario et al. also suggested that the quantity $\overline{v^3}$ should obtain negative values in the negative energy production region. Bario's suggestion was verified in the present work, where the terms $\overline{v^3}$ and $\overline{u^2v}$ were calculated for various (x, y) -positions. The negative signs of these terms in the negative energy production region, indicate that the mean turbulent kinetic energy is transferred from the wake flow towards the near wall region. Eskinazi and Erian [27] argued that for a fully developed turbulent flow in a pipe, the production term $-\overline{u_i u_j} \partial \overline{U_i} / \partial x_j$ has an opposite sign to the sign of the transfer term in the energy balance and the same sign with the dissipation term. In their study, the absolute values of the production term were always larger than those of the transfer term.

Brodkey et al. [28], suggested a different expression of the production term. They used the expression $-\overline{u_i u_j} \partial (\overline{U_i} + u_i) / \partial x_j$ instead of the $-\overline{u_i u_j} \partial \overline{U_i} / \partial x_j$ occurring in the turbulent energy conservation equation. This expression provides the possibility of relating the turbulent energy production to instantaneously occurring coherent structures responsible for the turbulent energy production. The new production term is the time average of the product of two instantaneously occurring quantities, i.e. $u_i u_j$ and $\partial (\overline{U_i} + u_i) / \partial x_j$; in this way it is compatible with the instantaneous production of turbulent kinetic energy and it has a direct physical meaning. Using the new production term, the instantaneous contributions of the quadrants have also always a physical meaning in time and space. For the proper substitution of the old by the new production term in the equation of the turbulent kinetic energy, Brodkey et al. used the following relation,

$$-\overline{u_i u_j} \frac{\partial (\overline{U_i} + u_i)}{\partial x_j} = -\overline{u_i u_j} \frac{\partial \overline{U_i}}{\partial x_j} - \frac{\partial \overline{u_i^2 u_j} / 2}{\partial x_j}. \quad (1)$$

In this way, the two production terms in equation (1) can be correlated when a turbulent kinetic energy transfer term is taken into account. If the $-\overline{u_i u_j} \partial \overline{U_i} / \partial x_j$ term is negative, the $-\overline{u_i u_j} \partial (\overline{U_i} + u_i) / \partial x_j$ term could be positive, only when both conditions below are satisfied:

$$-\frac{\partial \overline{u_i^2 u_j} / 2}{\partial x_j} > 0 \quad \text{and} \quad \left| \frac{\partial \overline{u_i^2 u_j} / 2}{\partial x_j} \right| > \left| \overline{u_i u_j} \frac{\partial \overline{U_i}}{\partial x_j} \right|. \quad (2)$$

Figure 7 shows the distribution of the sum $d\overline{v^3}/dy$ and $d\overline{u^2v}/dy$ in the y -direction at the streamwise distance $x = 120$ mm. Between the lines (1) and (2) extends the negative energy production region. It can be seen that, for the sum of these two gradients, both conditions (2) are satisfied in the negative energy production region.

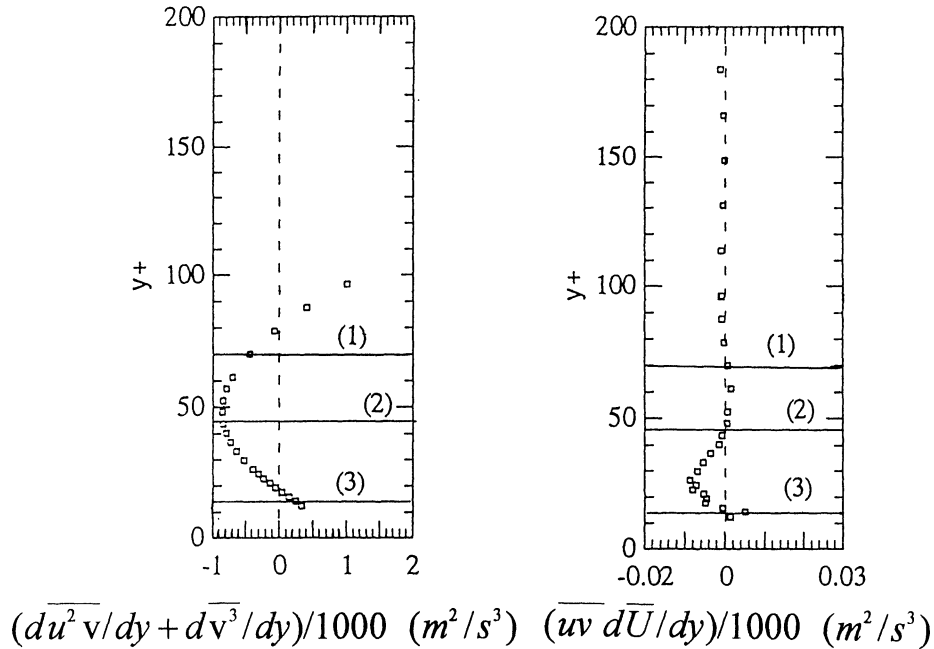


Figure 7. Distribution of the sum $d(u^2 v)/dy + d(v^3)/dy$ for the streamwise position $x = 120$ mm.

This result shows that in the negative energy production region, the new turbulent kinetic energy production term is positive. Hence, taking into account only the two transfer terms $d v^3/dy$ and $d u^2 v/dy$, the new energy production term, defined by Brodkey et al. [28] obtains positive values in the negative energy production region. This conclusion cannot be generally accepted, since the other transfer terms (e.g. $\partial(u^2 v/2)/\partial \chi$) should be also taken into account. This was not accomplished in the present work.

3.3. Quadrant splitting analysis

The purpose of this analysis was the association of certain elementary coherent structures with the process of turbulent energy production and transfer. For the investigation of the flow from the point of view of the coherent structures, one should look at the instantaneous fluid motions. Towards this direction, Wallace et al. [29] splitted the instantaneous $uv(t)$ signal into four quadrants, i.e.,

$$\text{Q1-quadrant (interaction outward): } u(t) > 0, v(t) > 0 (uv(t) > 0); \quad (3)$$

$$\text{Q2-quadrant (ejection): } u(t) < 0, v(t) > 0 (uv(t) < 0); \quad (4)$$

$$\text{Q3-quadrant (interaction wallward): } u(t) < 0, v(t) < 0 (uv(t) > 0); \quad (5)$$

$$\text{Q4-quadrant (sweep): } u(t) > 0, v(t) < 0 (uv(t) < 0). \quad (6)$$

Their names correspond to visually observed motions (elementary structures or events) in the wall region in fully developed pipe or channel flows. Wallace et al. [29] gave the percentage contributions $\overline{uv_Q}$, of each of the four quadrants (events) to the total Reynolds stress \overline{uv} , as a function of the distance from the wall, y^+ , in the case of a fully developed turbulent channel flow. In the present analysis, the $uv(t)$ signal was splitted in four quadrants, Q1, Q2, Q3 and Q4, according to the relations (3)–(6). A justification for applying this conditional

statistical analysis in this case is the belief that the inherent physics of bypass transition is similar to that of fully developed flow, rather than of natural transition (see also Voke and Yang [14])

The contribution of the quadrants, $\overline{uv_Q}$, to the total Reynolds stress can be non-dimensionalized by using the local sum of the absolute values of the contribution of the four quadrants, $\sum_{Q=Q_1}^{Q_4} |\overline{uv_Q}|$. In this dimensionless representation it is possible to observe directly the local activity of momentum flux due to every elementary coherent structure, relative to each other. *Figure 8* shows the normalized quadrant's contribution as a function of the y^+ distance for several x^+ positions, in the transition region. In the same figure and for the same x -positions, are presented the distributions of the local mean Reynolds stress, \overline{uv} , and the sum of the absolute values of the quadrant's contribution, $\sum_{Q=Q_1}^{Q_4} |\overline{uv_Q}|$, both normalized by the free stream kinetic energy per unit mass, $U_0^2/2$. From the distributions presented in *figure 8* and for the x -positions between the transition onset and $x = 100$ mm, two y^+ -regions can be identified; the wall region and the outer region. This distinction between the two regions was based on the different slope of the curves $\sum_{Q=Q_1}^{Q_4} |\overline{uv_Q}|$ as a function of y^+ . For example, at $x = 50$ mm ($x^+ = 875$), the wall region extends from the wall to a distance of $y^+ = 26$ and the outer region to y^+ greater than 26. At this streamwise position in the wall region, the contribution of the interactions outward to the local Reynolds stress is dominant. In the outer region ($y^+ > 26$), the contribution of the ejections and sweeps to the local Reynolds stress obtained low values, while the interactions wallward were the main contributors.

As can be observed in *figure 8*, in the first streamwise region (between $x^+ = 875$ and 1750), for each streamwise position in the wall region, the quantity $\sum_{Q=Q_1}^{Q_4} |\overline{uv_Q}|/(U_0^2/2)$ obtained a relatively constant value; this constant value, corresponding to each x -position, was continuously increasing with the streamwise distance. In the outer region, the values of $\sum_{Q=Q_1}^{Q_4} |\overline{uv_Q}|/(U_0^2/2)$ were gradually increasing with the y^+ -distance. This behaviour in the outer region can be attributed to the effect of the external von Karman structure. In the second streamwise region, which extends from $x^+ = 1750$ to 3500, the values of $\sum_{Q=Q_1}^{Q_4} |\overline{uv_Q}|/(U_0^2/2)$ were higher, compared to the ones in the first streamwise region; they also did not show a wall and an outer region character in the y -direction. In this region, the developing flow gradually approaches the character of a fully developed turbulent boundary layer. This can be verified by the contributions of the elementary coherent structures to the total Reynolds stress, which can be compared to the corresponding values given by Wallace et al. [29]. Furthermore, it is noted that in the outer region and also in the second streamwise region ($1750 < x^+ < 3500$), the interactions wallward have the higher contribution. For each x^+ -position in the first streamwise region, the y^+ -extent of the wall region, \mathcal{Y}_m^+ , was specified. It is observed that \mathcal{Y}_m^+ increases with x^+ , following the linear relation $\mathcal{Y}_m^+ = 0.021x^+$.

In what follows, an attempt will be presented to interpret the behavior of the quantity $\sum_{Q=Q_1}^{Q_4} |\overline{uv_Q}|/(U_0^2/2)$ in the transition region. The external von Karman wake provides the wall region with turbulent kinetic energy. This transfer takes place from the outer region. The high turbulence activity encountered in the wake is reflected here as a change in the slope of $\sum_{Q=Q_1}^{Q_4} |\overline{uv_Q}|/(U_0^2/2)$ as a function of y^+ in the outer region, in comparison to the same slope in the wall region. The increase, now, of the level of the $\sum_{Q=Q_1}^{Q_4} |\overline{uv_Q}|/(U_0^2/2)$ with x^+ in the wall region, is also attributed to that transfer of energy from the wake. The turbulent kinetic energy of the external wake decreases with the streamwise distance. At this point one could speculate that at some distance downstream from the transition onset, the kinetic energy of the wake is comparable to the kinetic energy of the wall region. At these streamwise positions, the slope of $\sum_{Q=Q_1}^{Q_4} |\overline{uv_Q}|/(U_0^2/2)$ as a function of y^+ decreases drastically; for the data presented here (*figure 8*), these streamwise distances are observed to be beyond 100 mm ($x^+ > 1750$).

In the present study of the strong wake induced boundary layer transition, the ejections and the interactions wallward were the main contributors to the total Reynolds stress, especially in the second streamwise region. In the first region of high contribution, $x_{\text{onset}}^+ < x^+ < 1750$, the interactions wallward were the main contributors,

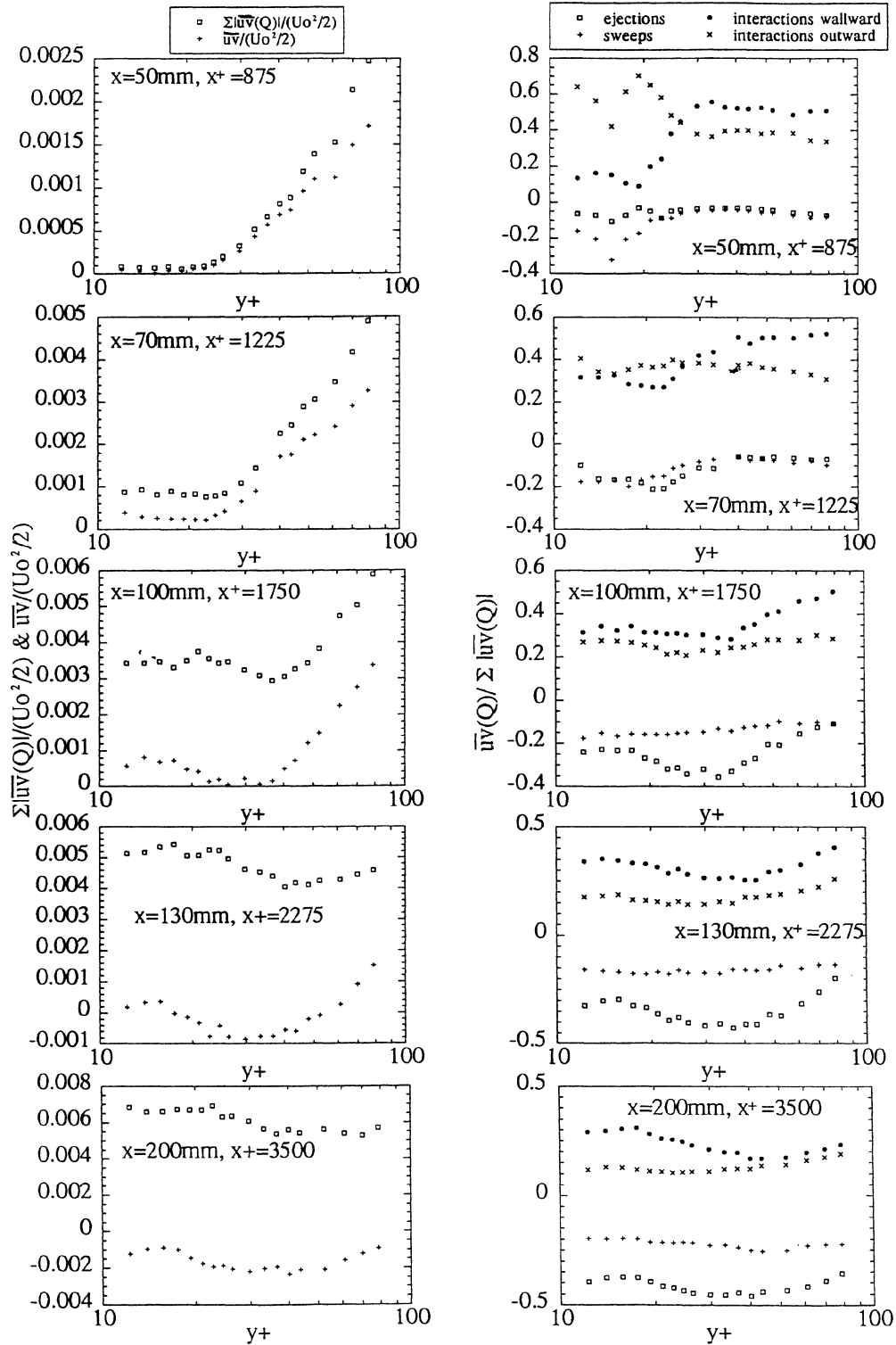


Figure 8. Distributions of $\overline{uv}/\sum_{Q=Q_1}^{Q_4} |\overline{uv}|$, $\sum_{Q=Q_1}^{Q_4} |\overline{uv}|/(U_0^2/2)$ and $\overline{uv}/(U_0^2/2)$ for various streamwise positions in the transition region.

while in the region $1750 < x^+ < 3500$, the contribution of the ejections was larger than that of the other quadrants. In contrast to the contributions of the above mentioned quadrants, sweeps and interactions outward obtained low values along the transition region. The changed role of the main contributors (ejections and interactions wallward), occurred gradually along the transition region and can also be observed in the y -direction. The interactions wallward obtained their maximum values in the negative energy production region, where the transfer terms were very strong, in contrast to the ejections, which they obtained their maximum values in the production region, close to the wall. The significant role of the ejections in the production process, is also manifested by the final increase of the production region thickness as a function of the streamwise distance x . On the other hand, the high contributions of the interaction wallward, which are negative contributors to the total Reynolds stress, create a balance between the transfer terms (interactions) and the production terms (mainly ejections). In the production region high contributions of all the quadrants were observed; the contributions of the ejections were the dominant. The initial development of the high contribution regions of the wall, was followed by the gradual shifting of these regions, to higher y -distances from the wall, as a function of the streamwise distance. These phenomena could be related to the development and lift-up of large scale secondary vortical structures, along the transition region (Kyriakides et al. [16]).

4. Conclusions

The flow characteristics during a bypass wake induced transition on a flat plate were experimentally investigated. In the streamwise region between $x^+ \approx 600$ and 1750 and in the normal to the wall direction, two distinct regions were identified; the wall region, where the sum of the absolute values of the contributions of the elementary quadrant events to the Reynolds stress, $\sum_{Q=Q_1}^{Q_4} |\overline{uv_Q}|/(U_0^2/2)$, were approximately constant and the outer region, where the same quantity increased linearly with the y^+ -distance. In the streamwise region between $x^+ = 1750$ and 3500, the quantity $\sum_{Q=Q_1}^{Q_4} |\overline{uv_Q}|/(U_0^2/2)$ obtained relatively constant values in the normal to the wall direction.

The profiles of the rms-values of streamwise and normal to the wall velocity fluctuations are nearly self-similar. The minima increase linearly with both streamwise and normal to the wall distances. This increase occurs up to $Re_x \approx 35000$ and $y^+ \approx 50$. A negative energy production region was identified along the transition region. The normal to the wall extent of this region up to a streamwise distance of 90 mm ($x^+ = 1575$) lies between the wall and a y -distance which increases with the streamwise position. Further downstream, the negative energy production region is located away from the wall at y -distances, which increase with the streamwise position. Furthermore, in the negative energy production region, the values of the calculated turbulent transfer terms, like $\overline{v^3}$ and $\overline{u^2v}$, indicate that turbulent kinetic energy is transferred in the normal to the wall direction, from the external wake towards the near wall region. It should be noted that the interactions wallward obtained their maximum values in the negative energy production region, where the transfer terms obtained high values, while the ejections obtained high values in the production region, close to the wall.

Acknowledgements

This work has been supported by BRITE/EURAM Area 3, Contract No. AERO-CT92-0050.

References

- [1] Squire L.C., Interactions between wakes and boundary layers, Prog. Aerospace Sci. 26 (1989) 261–288.
- [2] Schlichting H., Boundary Layer Theory, McGraw-Hill, New York, 1968.

- [3] Morkovin M.V., On the many faces of transition, in: Wells G.S. (Ed.), *Viscous Drag Reduction*, Plenum Press, New York, 1969, pp. 1–31.
- [4] Kachanov Y.S., Physical mechanisms of laminar boundary layer transition, *Annu. Rev. Fluid Mech.* 26 (1994) 411–482.
- [5] Mayle R.E., The role of laminar-turbulent transition in gas turbine engines, *ASME-Paper* 91-GT-261, 1991.
- [6] Schubauer G.B., Skramstad H.K., *Laminar boundary layer oscillations and transition on a flat plate*, NASA-Report 909, 1948.
- [7] Nishioka M., Morkovin M.V., Boundary layer receptivity to unsteady pressure gradients: experiments and overview, *J. Fluid Mech.* 171 (1986) 219–261.
- [8] Goldstein M.E., Hultgren L.S., Boundary-layer receptivity to long-wave free-stream disturbances, *Annu. Rev. Fluid Mech.* 21 (1989) 137–166.
- [9] Westin K.J.A., Boiko A.V., Klingmann B.G.B., Kozlov V.V., Alfredsson P.H., Experiments in a boundary layer subjected to free stream turbulence. Part I: Boundary layer structure and receptivity, *J. Fluid Mech.* 281 (1994) 193–218.
- [10] Westin K.J.A., Bakchinov A.A., Kozlov V.V., Alfredsson P.H., Experiments on localized disturbances in a flat plate boundary layer. Part I: The receptivity and evolution of a localized free stream disturbance, *Eur. J. Mech. B-Fluid.* 17 (1998) 823–846.
- [11] Buter T.A., Reed H.L., Boundary layer receptivity to free-stream vorticity, *Phys. Fluids* 6 (1994) 3368–3379.
- [12] Morkovin M.V., Reshotko E., Dialogue on progress and issues in stability and transition research, in: Arnal D., Michel M. (Eds), *Proc. IUTAM Symp. on Laminar-Turbulent Transition*, Springer-Verlag, France, 1990, pp. 3–29.
- [13] Savill A., Zhou M., Wake/boundary layer and wake/wake interactions-smoke flow visualization and modeling, in: Ko N.M.C. (Ed.), *Proceedings of the 2nd Asian Congress of Fluid Mechanics*, Beijing, China, Science Press, 1983, pp. 743–754.
- [14] Voke P.R., Yang Z., Numerical study of bypass transition, *Phys. Fluids* 7 (1995) 2256–2264.
- [15] Kyriakides N.K., Kastrinakis E.G., Nychas S.G., Goulas A., Prediction of boundary layer transition induced by a von Karman vortex street wake, *J. Aerosp. Eng.* 210 (1996) 167–179.
- [16] Kyriakides N.K., Kastrinakis E.G., Nychas S.G., Goulas A., Aspects of flow structure during a cylinder wake induced laminar/turbulent transition, *AIAA J.* 37 (1999) 1197–1205.
- [17] Van Atta C., Gharib M., Ordered and chaotic vortex streets behind circular cylinders at low Reynolds numbers, *J. Fluid Mech.* 174 (1987) 113–133.
- [18] Wills J.A.B., The correction of hot-wire readings for proximity to a solid boundary, *J. Fluid Mech.* 12 (1962) 388–396.
- [19] Oka S., Kostic Z., Influence of wall proximity on hot-wire velocity measurements, *DISA-Information* 13 (1972) 29–33.
- [20] Eckelmann H., Nychas S.G., Brodkey R.S., Wallace J.M., Vorticity and turbulence production in pattern recognized turbulent flow structures, *Phys. Fluids* 20 (1977) S225–S231.
- [21] Vukoslavcevic P., Wallace J.M., Influence of velocity gradients on measurements of velocity and streamwise vorticity with hot-wire X-array probes, *Rev. Sci. Instrum.* 52 (1981) 869–879.
- [22] Kastrinakis E.G., Eckelmann H., Measurement of streamwise vorticity fluctuations in a turbulent channel flow, *J. Fluid Mech.* 137 (1983) 165–186.
- [23] Hall A.A., Hislop G.S., Experiments on the transition of the laminar boundary layer on a flat plate, *ARC R & M* (1938) 1843.
- [24] Cimbala J.M., Nagib H.M., Roshko A., Large structure in the far wakes of two dimensional bluff bodies, *J. Fluid Mech.* 190 (1988) 265–298.
- [25] Pfeil H., Herbst R., Schroeder T., Investigation of the laminar/turbulent transition of boundary layers disturbed by wakes, *J. Eng. Gas Turb. Power* 105 (1983) 130–137.
- [26] Bario F., Charnay G., Papailiou K.D., An experiment concerning the confluence of a wake and a boundary layer, *J. Fluid. Eng.* 104 (1982) 18–24.
- [27] Eskinazi S., Erian F.F., Energy reversal in turbulent flows, *Phys. Fluids* 12 (1969) 1988–1998.
- [28] Brodkey R.S., Nychas S.G., Taraba J.L., Wallace J.M., Turbulence energy production, dissipation and transfer, *Phys. Fluids* 16 (1973) 2010–2011.
- [29] Wallace J.M., Eckelmann H., Brodkey R.S., The wall region in turbulent shear flow, *J. Fluid Mech.* 54 (1972) 39–48.